Journal of Materials and Environmental Science
ISSN : 2028-2508
e-ISSN : 2737-890X
CODEN : JMESCN
Copyright © 2026,

J. Mater. Environ. Sci., 2026, Volume 17, Issue 10, Page 1548-1568

http://www.jmaterenvironsci.com

Effect of purification and acid activation on two clays from Côte d'Ivoire, swelling (Katiola) and non-swelling (Dabou): Studies by ICP, DRX, BET and CEC for their valorization in adsorption

Adjoumani Yao Joseph [1*], Abro Koutouan Désiré Martial [1], Djassou Adjoavi Colette [1,2], Sanou Ali [1,3] ; Yao Kouassi Benjamin [1]**

[1]Laboratoire des Procédés Industriels de Synthèses, de l'Environnement et des Energies Nouvelles (LAPISEN), Institut National Polytechnique Félix Houphouët-Boigny (INP-HB), BP 1093 Yamoussoukro, Côte d'Ivoire
[2]Ecole d'Ingénieurs de Construction Navale, Université de San-Pédro (USP), BP 1800 San-Pédro, Côte d'Ivoire
[3]Laboratoire des Sciences Physiques Fondamentales et Appliquées (LSPFA), Ecole Normale Supérieure (ENS), 08 BP 10, Abidjan, Côte d'Ivoire
**Corresponding author, Email address: yao.adjoumani@inphb.ci*
***Corresponding author, Email address: benjamin.yao@inphb.ci*

Received *14 Aug 2026,*
Revised *23 Oct 2026,*
Accepted *26 Oct 2026*

Keywords:
- ✓ *Clay;*
- ✓ *Acid activation;*
- ✓ *Specific surface area;*
- ✓ *Interfoliar space*

Citation*: Adjoumani Y. J., Abro K. D. M., Djassou A. C. Sanou A. Yao K. B. (2026) Effect of purification and acid activation on two clays from Côte d'Ivoire, swelling (Katiola) and non-swelling (Dabou): Studies by ICP, DRX, BET and CEC for their valorization in adsorption, J. Mater. Environ. Sci., 17(10), 1548-1568*

Abstract: In this study, the effect of purification and acid activation on two Ivorian clays (Dabou and Katiola) was investigated. The clays were washed and purified to achieve a particle size fraction of less than 50 µm (K50 and D50) and 2 µm (K2 and D2), respectively. The purified clay was then activated with acid (K2A and D2A). Chemical, mineralogical, and textural changes were examined using ICP spectroscopy, X-ray diffraction (XRD), BET, and cation exchange capacity (CEC). The results revealed that the two samples are aluminosilicates of very different natures. The purified clay from Dabou (D2) is rich in kaolinite (66.4%) followed by illite (20.3%) as clay minerals, while that from Katiola (K2) is mainly composed of smectite (51.9%), particularly montmorillonite, with a significant kaolinite content (39.3%). Both samples are mesoporous with the presence of micropores. However, the Dabou clay (D50) has a lower specific surface area and CEC compared to that from Katiola (K50). The treatments performed allowed for the removal of a large portion of the impurities contained in the samples and increased their specific surface area, as well as the volume and size of the pores. The cation exchange capacity and specific surface area increased more in the case of the Katiola clay (K2). The overall results show that while purification improves the properties of both samples, acid activation optimizes the surface area and CEC of the Katiola clay, but destroys the structure of the Dabou clay through leaching. The samples can be used as adsorbents for pollutant removal in aqueous environments. However, the swelling Katiola clay appears to be the best candidate for adsorption applications in its purified and activated form (K2A).

1. Introduction

Clay materials arouse major industrial and scientific interest due to their abundance and especially their physicochemical properties, such as their cation exchange capacity, their specific surface area, their porosity and their plasticity (Bergaya and Lagaly, 2013; Dehmani *et al.*, 2026). However, in the raw state, clays often contain crystalline impurities (quartz, carbonates, iron oxides) or secondary phases (goethite, tobermorite) which limit their performance (Murray, 2007). To optimize their environmental and industrial applications-particularly for pollutant adsorption processes - structural and surface modifications are essential.

The present study is part of this optimization approach by evaluating the impact of two distinct valorization techniques: purification and acid activation (Haoufazane *et al.*, 2025). The work focuses on two materials with very different mineralogical compositions: a first sample mainly made up of smectite associated with a minor fraction of kaolinite, and a second sample rich in kaolinite with a secondary phase of illite.

The main objective is to identify and compare the structural, textural and compositional mutations induced by these treatments on these two types of clay matrices. To do this, an analytical approach is deployed through four fundamental characterization techniques:

• Chemical analysis by ICP will make it possible to follow the evolution of the overall elemental composition and to quantify the leaching rate of structural cations during acid attack (Christidis *et al.*, 1997; Komadel and Madejová, 2006).

• X-ray Diffraction (XRD) will be used to identify crystallographic transformations, to verify the impact of treatments on the interfoliar space of smectite and on the structural network of kaolinite and illite (Bish and Post, 1989).

• Measuring Cation Exchange Capacity (CEC) will assess changes in surface reactivity (Bergaya and Lagaly, 2013).

• Textural analysis by BET will make it possible to precisely quantify the increase in specific surface area and the development of porosity, essential for adsorption performance (Komadel and Madejová, 2006).

Through the comparison of these results, this work will highlight the fundamental mechanisms which govern on the one hand the elimination of the associated phases by purification, and on the other hand the collapse or structural reorganization by acid activation, in order to correlate these modifications with their final efficiency in adsorption.

2. Materials and methods

2.1. Clay raw materials

The clays used in this study come from two different clay sites in Côte d'Ivoire, namely Katiola and Dabou. **Table 1** gives the geographical coordinates of the sites. The samples were extracted in the form of blocks and placed in new polyethylene bags to be transported to the laboratory for analysis. Before any analysis, these raw samples were dried at room temperature for 72 hours, crushed, ground and then stored in polyethylene bags.

Table 1. GPS coordinates of clay sites

Sample codes	Localities	Coordinates	
		Latitude	Longitude
K	Katiola	08°08' N	05°05' W
D	Dabou	05°15' N	04°20' W

2.2 Washing and purification of clays

Two clay fractions (50 µm and 2 µm) were produced from each sample. The first fraction (50 µm) is obtained by wet sieving. To do this, a mass of raw clay, initially dried, crushed and ground, is soaked in a tank of water for 24 hours to break up the lumps of clay and separate them from the earth.

The contents of the tank are then poured onto a column of sieves with different opening diameters, arranged one on top of the other in decreasing order of mesh, the last of which is the 50 µm sieve (**Figure 1a**). Under the effect of the water current, the passage of particles is facilitated using a

brush. The phase thus obtained is dried in an oven at 105 °C for 24 h and constitutes the washed clay (**Figure 1b**). The powders obtained are noted D50 for the Dabou sample and K50 for that of Katiola.



Figure 1. (a) wet sieving on a sieve column to obtain clay fractions < 50 µm; (b) oven drying at 105 °C

The 2 µm fraction is extracted from the first in accordance with the protocol of Thiry et al. (Thiry *et al.*, 2013). It is carried out in four stages. First of all, there is the destruction of organic matter in the clays resulting from the first clay phases (D50 and K50) under the action of hydrogen peroxide (H_2O_2). Then, the elimination of carbonates ($CaCO_3$) with hydrochloric acid. Subsequently, the clay particles are dispersed using a dispersing agent such as sodium chloride. Finally, the particle size of 2 µm constituting the purified clay is obtained by siphoning and drying the supernatant of a test tube, on the upper 2/3 after 24 hours of sedimentation according to Stokes' law (**Figure 2**). The Katiola sample is denoted K2 and that of Dabou D2.

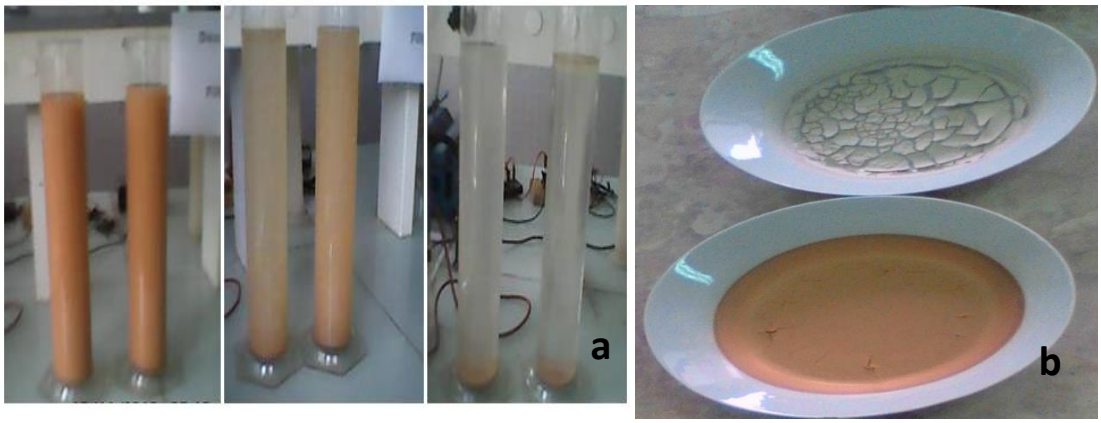


Figure 2. (a) State of the liquid after 2 weeks of siphoning to obtain pure clay; (b) Samples of Katiola clay (yellow-orange color) and Dabou clay (light gray color) after drying in an oven at 105 °C

2.3 Activation of clay samples

Activation of the clays was carried out with 2 N sulfuric acid. Activation is carried out in a 500 cm^3 three-layer flask, equipped with a condenser, a magnetic stirrer, a magnetic bar and a thermometer (**Figure 3**). The mass of clay to activate and the mass of acid to use are determined in a clay/acid ratio of 1:7.5 (Seghairi and Achour, 2003). The mixture is heated to 100 °C throughout the activation (16 h) using a water bath or a heat transfer oil bath into which the reactor is immersed.

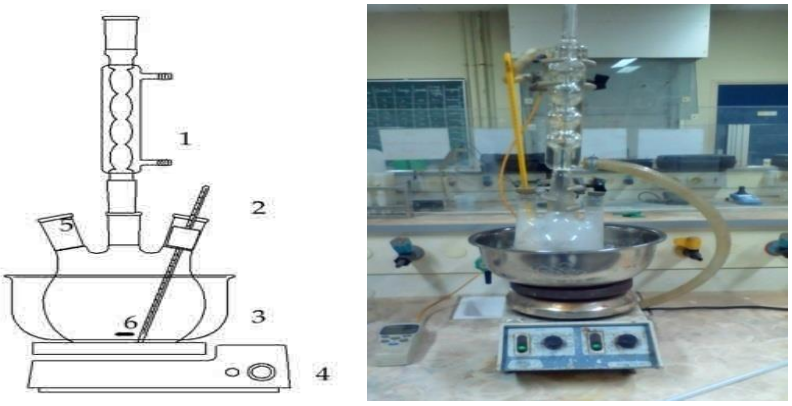


Figure 3. Device for activation (1-refrigerant; 2-thermometer; 3-water bath; 4-stirring hot plate; 5-tripole flask; 6-magnetic bar)

2.4 Chemicals

The chemicals used were all of analytical grade. They were obtained commercially and used without any purification. These are sodium chloride (NaCl), hydrochloric acid (HCl, 37%) and hydrogen peroxide (H_2O_2, 50%) which were purchased from Merck (Germany). Sulfuric acid (H_2SO_4, 95-97%, d = 1.86) came from CHEM-LAB. The solutions were all prepared with distilled water.

2.5 Clays characterization methods

Various characterization techniques were used in this work to determine the mineralogy, structural and textural properties of the clays.

2.5.1 X-ray diffraction

X-ray diffraction (XRD) was carried out on the disoriented powders using a diffractometer comprising a Debye-Scherrer assembly, operating in reflection, equipped with an INEL CPS 120 curved detector and an X-ray source using Kα radiation from copper of wavelength λ = 1.54060 Å and operating at 30 kV and 15 mA. The surveys are carried out in the angular interval 0 – 70° in 2θ with a step of 0.02° and an X-ray photon counting time of 2 s per step. Software associated with the diffractometer identifies the clay and crystalline phases. The quantification of the different minerals present in the clays was done using appropriate software coupled with the database of the International Center for Diffraction Data (ICDD). The XRD was carried out at INP Grenoble in France, at the Center for Common Technical Means (CMTC).

2.5.2 Chemical characterization

Chemical analysis of the samples was carried out on the powders using an Agilent 720 ES type device equipped with an ICP-AES plasma (Inductively Coupled Plasma – Atomic Emission Spectroscopy). It consisted of determining the content of silica and major elements by ICP-AES, and that of trace elements by ICP-MS (Inductively Coupled Plasma-Mass Spectroscopy). The quantities measured are expressed as a percentage of oxide relative to the weight of the sample. The chemical analysis was carried out at the Laboratory of Thermodynamics and Physico-Chemistry in Metallurgy (LTPCM) at INP Grenoble in France.

2.5.3 Determination of specific surface area and texture

The specific surface area as well as pore characteristics of the clay materials were determined by the Brunauer–Emmett–Teller (BET) method on samples decontaminated of any traces of moisture or other adsorbents, using a Quantachrome Autosorb-6B surface and porosity analyzer (N_2 or CO_2).

The method is based on determining the volume of nitrogen necessary to form a monolayer of molecules of this gas on the surface of clay at 77 K, the temperature at which nitrogen is liquid and under normal atmospheric pressure. Pore volume and diameter were also determined. Adsorption–desorption isotherms were measured near the boiling point of nitrogen (77 K). The gas pressure was gradually increased to the saturation value, when condensation of the adsorbate (N_2) occurred in the powder pores. The BET analyzes were carried out at INP Grenoble in France, at the Earth Sciences Laboratory (SiTerre).

2.5.4 Cation exchange capacity

The cobaltihexamine method was used to determine the cation exchange capacity (CEC) of clays (Mantin and Glaeser, 1960). This method consists of measuring by colorimetry the concentration of cobaltihexamine ions remaining in the supernatant after adsorption by the clays using UV-visible spectrometry.

To do this, 2.5 g of clay are brought into contact with 50 mL of 0.05 N solution of cobalthexamine ion and the mixture is stirred for 2 h using a rotary stirrer; centrifuged at 6000 rpm for 15 minutes and filtered through a membrane with a porosity of 0.45 µm. The concentration of cobaltihexamine ion in the filtrate is subsequently determined spectrophotometrically with a UV-visible spectrophotometer (JASCO V-530) by measuring the absorbance (A_{475}) in the visible ($\lambda = 475$ nm) where the adsorption band is maximum. This concentration is obtained using a calibration line previously drawn with standard solutions (0.0125 N; 0.025 N; 0.0375; 0.05 N) of cobaltihexamine. The mathematical formula given by **Eqn. 1** makes it possible to determine the CEC in meq/100 g of sample. The determination of the CEC was carried out at the Laboratory of Industrial Processes, Synthesis and New Energies (LAPISEN) of the INP HB in Yamoussoukro in Côte d'Ivoire.

$$\boldsymbol{CEC = \left(N_i - N_f\right) \times \frac{V}{m} \times 100} \qquad \textbf{Eqn. 1}$$

With
Ni: initial normality in cobaltihexamine (0.05 N);
Nf: residual normality;
V: volume of the solution (50 mL);
m: mass of the clay sample (2.5 g).

3. Results and Discussion

3.1 Characteristics of raw and purified clays

In this part, we show the results of chemical, mineralogical and textural analyzes of raw clays with a grain size of 50 µm and those purified with a grain size of 2 µm. The objective here is to show the effect of treatment by purification of clays.

3.1.1 Chemical composition

The chemical composition of the clay samples in terms of oxides is presented in **Table 2**.

Table 1. Chemical composition of clays expressed in % by mass of oxides

	SiO_2	Al_2O_3	Fe_2O_3	K_2O	MgO	CaO	Na_2O	MnO	TiO_2
K50	44.97	16.06	23.84	0.57	3.72	0.74	0.45	0.02	0.55
K2	38.18	17.46	16.13	0.16	6.64	3.75	4.44	0.00	0.30
D50	81.07	15.37	3.5	1.89	0.31	0.17	0.11	0.03	0.21
D2	55.83	34.84	2.13	1.75	0.20	0.30	0.19	0.00	0.14

Concerning the Katiola K50 sample, the results indicate that the main oxides which constitute it are silica (SiO_2), alumina (Al_2O_3) and iron oxide (Fe_2O_3), with respective contents of 44.97; 16.06 and 23.84%. Magnesium oxide (MgO) is found in reduced quantities. The oxides of sodium (Na_2O), calcium (CaO), potassium (K_2O) and titanium (TiO_2) appear in more reduced forms while manganese oxide (MnO) is in trace form. Such an observation suggests, according to Boulingui et al., that the extraction deposit of this clay would have reached maturity (Boulingui *et al*., 2015). The high level of silica (SiO_2) and alumina (Al_2O_3) shows that the K50 sample contains aluminosilicates (Amari *et al*., 2018; Rehman *et al*., 2021; Soro *et al*., 2023; Soro *et al*., 2026; El Bourachdi *et al*., 2027). The high content of iron (III) oxide shows that the Katiola clay is ferric and could therefore contain goethite (Nshimiyimana *et al*., 2020), the origin of its yellow coloring (Sako *et al*., 2025; Tra *et al*., 2026).

The transition from K50 to K2 after sodium treatment and sedimentation results in a reduction in the SiO2 level from 44.97 to 38.18%; indicating a probable elimination of silica in the form of quartz. This treatment is also accompanied by a relative reduction of nearly 32.4% in iron (III) oxide due to possible elimination of goethite. The increase in the level of magnesium oxide (MgO) would presage the existence of clay minerals having magnesium and iron as structural cations in substitution with aluminum in the octahedral sites (O) or also with silicon in the tetrahedral sites (T) for iron. Their permanent presence with these possibilities of isomorphic substitutions suggests the existence of 2:1 type clay minerals at the Katiola clay level (Alujas *et al*., 2015; Neji *et al*., 2009). The sodium level, for its part, increases almost 10 times following sodium treatment. This means that the objective of sodium enrichment of the interfoliar space of the clay with a view to facilitating ionic exchanges when necessary has been achieved. Gueu et al., who worked on the same sample, reported a similar result after sodium treatment, with an increase from 0.04% to 1.94% (Gueu *et al*., 2019). Furthermore, several studies have indicated a notable increase in Na_2O levels after sodium treatment (Gauly *et al*., 2025; Ourari *et al*., 2018).

Concerning Dabou clay, the results of sample D50 show that the main oxides present in Dabou clay are SiO_2 and Al_2O_3. Iron oxide is found there in small quantities compared to Katiola clay. The light gray coloring presented by the Dabou clay indicates that the iron there is more in the form of ferrous ions (Ségalen, 1969). The constant presence of potassium oxide (K2O) in the two samples D50 and D2, even with an average quantity of 1.8%, would reflect the existence of a micaceous phase such as illite in the Dabou sample Dabou (Alujas *et al*., 2015; Garba Labo *et al*., 2026). The other oxides, calcium, magnesium, sodium and titanium, are in lower quantities and would indicate that the Dabou site would also be mature (Boulingui *et al*., 2015).

These first analyzes do not suggest isomorphic exchanges as was perceived in the case of Katiola clay. In addition, the sodium treatment did not cause a strong change in the sodium oxide level as in the case of Katiola clay. The rate increased barely from 0.11 to 0.19% probably thanks to the slight decrease in potassium. Concerning silica, a relative decrease in the rate of 31.25% is observed when going from D50 to D2 showing an elimination of quartz after sedimentation.

The structural modifications linked to changes in the chemical composition following the different treatments will be studied in more detail using XRD, as well as their textural properties, namely the S_{BET} specific surface area, the size and volume of the pores.

3.1.2 Mineralogical composition of clays

The X-ray Diffraction results of the Katiola samples are given in **Figures 4** and **5**. Analysis of the diffractogram of K50 clay (Figure 4) reveals the presence of crystalline phases essentially in the form of kaolinite (7.19 Å at 12.3° and 3.5 Å at 25°, 2.42 Å at 37° and 1.97 Å at 46°) and smectite

(14.48 Å at 6.1°) as minerals. clayey, associated with impurities consisting of quartz (4.28 Å at 20.7° and 3.33 Å at 26.7° and 1.82 Å at 50°), goethite (4.22 Å at 21°, 2.44 Å at 36.8°, 1.66 Å at 55° and 1.48 Å at 62.5°) and tobermorite which is a hydrated calcium silicate located at 37° for a distance of 4.13 Å.

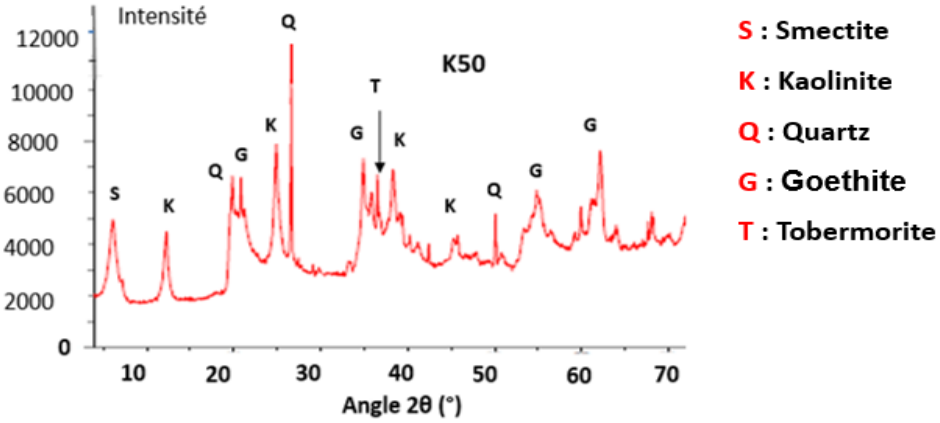


Figure 1. XRD of Katiola K50 clay (50 µm)

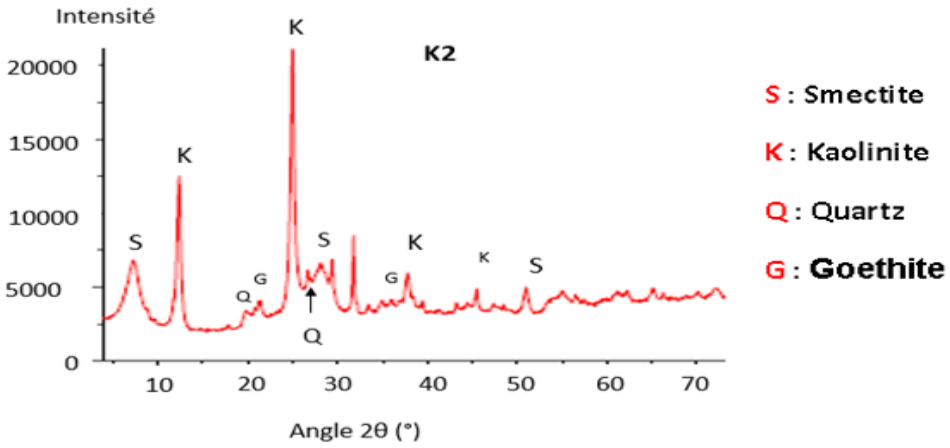


Figure 5. XRD of Katiola K2 clay (2 µm)

According to the work of Kpangni et al. and Gueu et al., the smectite present in the Katiola sample is montmorillonite (Gueu *et al.*, 2019; Kpangni *et al.*, 2008). The transition from K50 to K2 after sodium treatment and sedimentation (Figure 5), shows a strong reduction or disappearance of the impurity peaks: quartz at 20.7°, 26.7° and 50°, goethite at 21°, 36.8, 55 Å and 62.5 Å. The tobermorite at 37° has disappeared. Conversely, the kaolinite peaks located at 12.3° and 25° are intensified. The base line of smectite initially at 6.15° experiences a shift towards a larger angle equal to 7.25° corresponding to a smaller reticular distance, equal to 12.18 Å according to the zoom in **Figure 6**. This contraction observed in most works concerning the homoionization of smectite-type clays (Adjia, 2012; Bouras, 2003; Kpangni *et al.*, 2008) would be attributed to the departure of exchangeable cations such as hydrated Mg^{2+} housed in the interlayer space, and which are replaced by sodium ions following sodium treatment. The hydrated radius of sodium ions being smaller than that of magnesium ions, the interticular distance was reduced.

This possibility of variation in the intersheet distance shows that the Katiola clay is a swelling clay given the presence of the smectite it contains (Caillère *et al.*, 1982). The disappearance of almost all of the impurities shows that the sodium treatment and sedimentation carried out contribute to purifying the Katiola clay. The diffractograms of Dabou clay are presented in Figures 7 and 8, respectively for sample D50 and for sample D2.

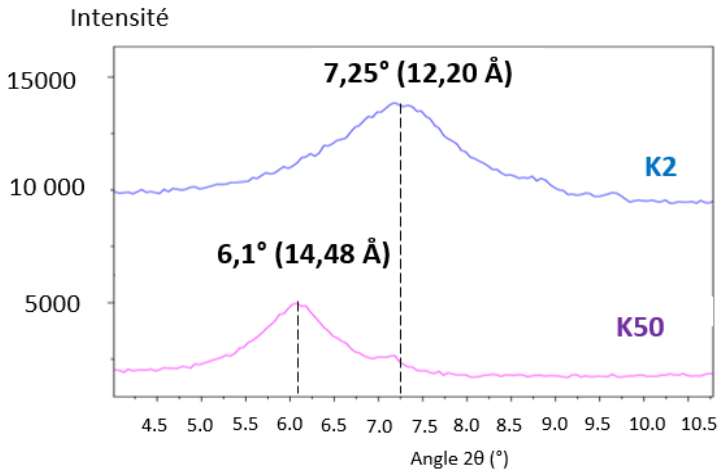


Figure 6. Zoom of the basic lines of smectite in the case of Katiola clays (K50 and K2)

Figure 7 reveals the presence of kaolinite (7.19 Å at 12.3° and 3.5 Å at 25°) and illite identified at 8.8° for a lattice distance equal to 10.04 Å Å (Emeruwa *et al.*, 2008; Meite *et al.*, 2018). Quartz identified at 20.7°; 26.7°; 36.5°; 39.5°; 42.5° and 45.9° appears as the only impurity.

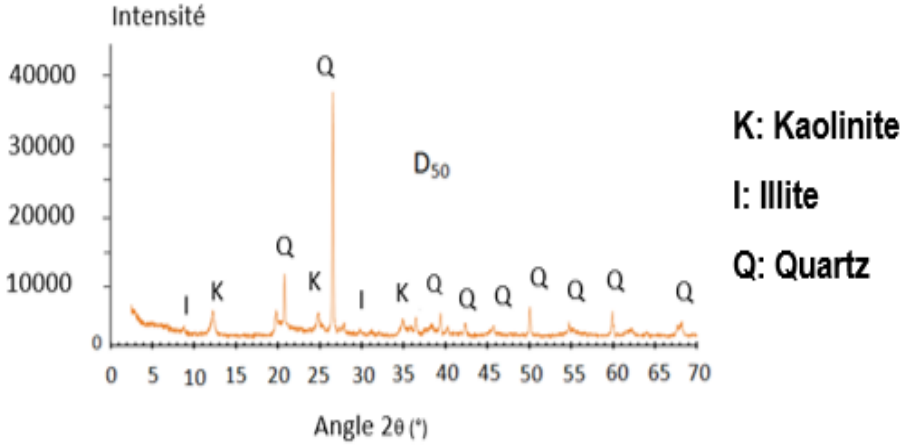


Figure 7. XRD of Dabou D50 clay (50 µm)

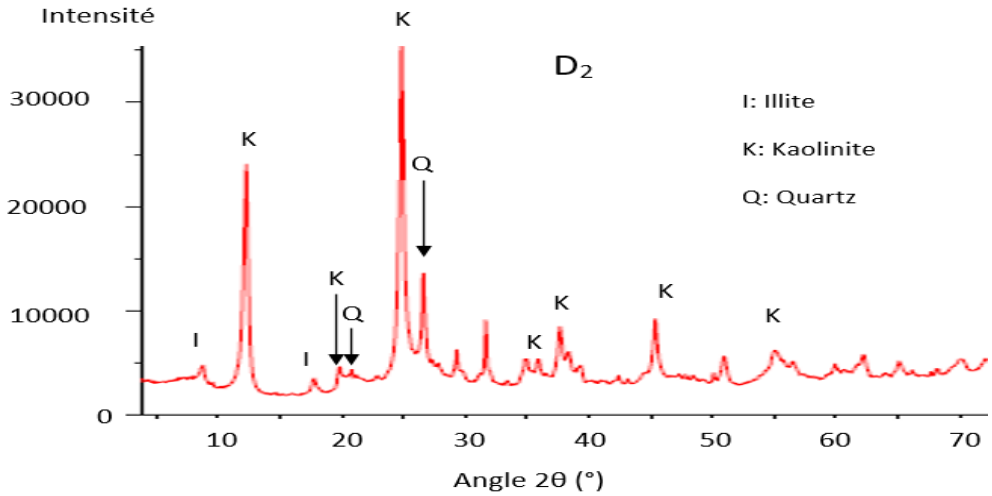


Figure 8. XRD of Dabou D2 clay (2 µm)

After sodium treatment and sedimentation, the diffractogram of sample D2 (**Figure 8**) shows that the quartz peaks all decreased in intensity; those of kaolinite, previously identified, became more intense and new lines appeared for illite, notably the line at 2θ = 17.7°. This intensification of the lines

of clay minerals to the detriment of quartz shows that treatment by sedimentation also allows purification of Dabou clay. Kaolinite was identified in the samples studied. It is a mineral generally found in clays originating from Côte d'Ivoire (Fort *et al*., 2024; Kouadio *et al*., 2022; Kouakou *et al.*, 2023; Méité *et al*., 2024; Sako *et al*., 2025; A. Sanou *et al*., 2024; Tra *et al*., 2026). It should be noted that there was no movement of rays for this Dabou clay. Which denotes that it is a non-swelling clay.

The mineralogical composition of the clays is given in **Table 3**. This table confirms that the purified clay of Katiola (K2) is very rich in smectite (51.9%) and the clay mineral associated with it is kaolinite (39.7%). The sedimentation treatment effectively reduced the impurities it contained (quartz, goethite and tobermorite). The same goes for Dabou clay (D2), rich in kaolinite (66.4%) accompanied by illite (20.3%) as a clay mineral. It ultimately appears that the purified clays (K2 and D2) are richer in clay minerals (kaolinite, illite and montmorillonite) than the raw clays (K50 and D50).

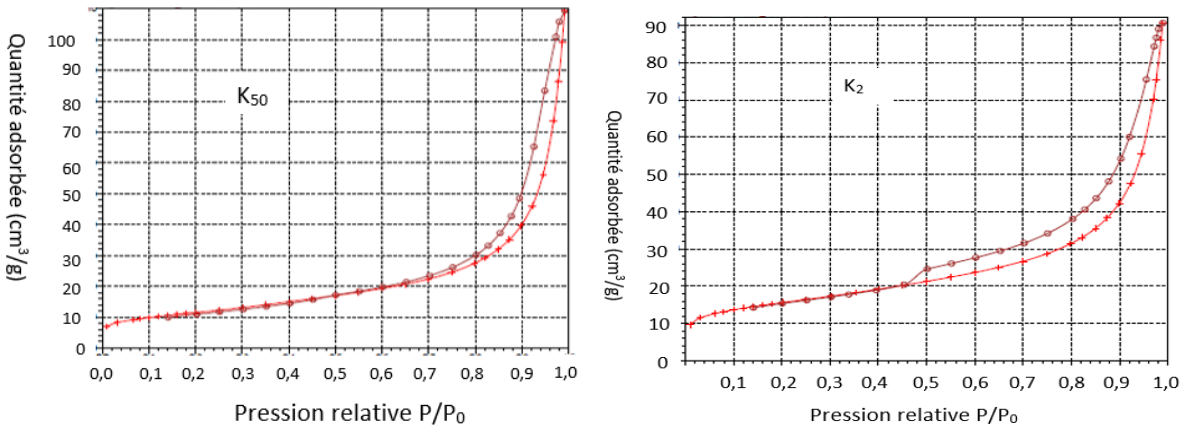
Table 2. Mineralogical composition of clay samples

	Minerals (%)					
Samples	**Quartz**	**Smectite**	**Kaolinite**	**Illite**	**Goethite**	**Tobermorite**
K50	20.7	33.2	29.1	–	16.2	0 ?8
K2	6.3	51.9	39.7	–	2.1	–
D50	67	–	17	16	–	–
D2	13.3	–	66.4	20.3	–	–

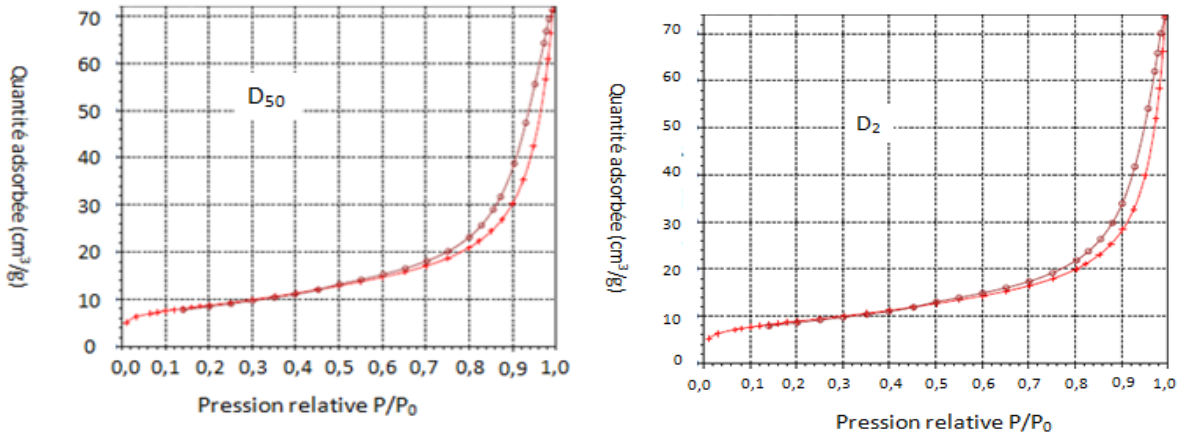
3.1.3 BET analysis

Textural properties, SBET as well as pore size distribution and volume were determined by N_2 physisorption at -196 °C. The nitrogen adsorption/desorption isotherms at 77 K are given in **Figures 9** and **10**. In each of these figures, two typical areas of relative pressure appear:

- the first domain, corresponding to a relative pressure between 0 and 0.45 approximately, describes the adsorption of a monolayer of gas on the external surfaces and the filling of micropores with openings ranging from 0 to 2 nm (Amari *et al*., 2018; Kpangni, 2009).
- the second domain, with a relative pressure P/P0 between 0.45 and 0.98 describes a multilayer adsorption, followed by capillary condensation with desorption revealing a hysteresis loop joining that of adsorption for P/P_0 greater than or equal to 0.45. This form of isotherm, type IV in the classification of the International Union of Pure Applied Chemistry, is characteristic of mesoporous solids (Sing *et al*., 1982). All the specific surface area, volume and pore size values for D50, D2, K50 and K2 are presented in **Table 4**.



Figures 9. N_2 adsorption-desorption isotherm of Katiola clay K50 and K2



Figures 10. N_2 adsorption-desorption isotherm of Dabou clay D50 and D2

This table shows that these clay materials studied are all mesoporous given the diameter of their pores, between 2 and 50 nm and also the total volume of the pores barely exceed 0.1 cm^3/g, as reported by Dubinin (Dubinin, 1979). The existence of specific surfaces and additional microporous volume confirms that these materials are indeed micro and mesoporous in accordance with the isotherms obtained. The effectiveness of an adsorbent material is essentially oriented towards its surface, both internal and external. Indeed, the higher the specific surface area of a material, the more it has the possibility of spreading sufficiently while occupying more space, thus allowing a significant accumulation of a given substance (I. Sanou *et al.*, 2026). This table also shows that purification increases the specific surface area, the pore diameter and the pore volume of these minerals. This could be due to the sodium treatment, the effect of which is to facilitate the dispersion of clay particles which may still be agglomerated after wet sieving. Surez et al., Nguetnkam et al. and Gauly et al. having also made this observation, attribute it to the departure of amorphous silica or to that of the impurities in which the clay would be buried; and the consequence of which is to cause openings and promote the creation of mesopores due to dispersion (Gauly *et al.*, 2025; Nguetnkam *et al.*, 2011; Surez *et al.*, 1995). This table ultimately shows that the specific surface area as well as the total pore volume of Katiola clay are greater than that of Dabou. This result is in agreement with their mineralogical composition since smectites are known to have a greater specific surface area and larger pore volume than kaolinite (Decarreau, 1990; Morgan *et al.*, 1985).

Table 4. Values of specific surface areas and pore volume of the clays used

	Micropore surface (m^2/g)	External surface (m^2/g)	BET specific surface (m^2/g)	Pore diameter (nm)	Micropore volume (cm^3/g)	Total volume (cm^3/g)
D50	3.82	27.63	31.45	11.14	$1.5.10^{-3}$	0.087
D2	3.24	33.76	37.00	12.11	$1.1.10^{-3}$	0.114
K50	12.24	43.21	55.45	7.84	$5.2.10^{-3}$	0.109
K2	9.07	48.02	57.09	9.29	$3.8.10^{-3}$	0.125

3.1.4 Cation exchange capacity

The cation exchange capacity (CEC) representing the total quantity of exchangeable cations that the clay can retain on its surface by electrostatic force at a given pH was determined (Gauly *et al.*, 2025; Rehman *et al.*, 2021). The CEC values obtained are mentioned in **Table 5**.

Table 3. Cation exchange capacity of the clays studied

CEC values	Samples			
	D50	D2	K50	K2
CEC (meq/100g)	14	16,7	37,5	51,5

This table shows that raw Dabou clay (D50) has a CEC value of 14 meq/100 g while purified clay (D2) has a value of 16.7. The CEC of D50 is included in the standard CEC value range indicated for kaolinite (3 – 15 meq/100g) but that of D2 is higher than this range while remaining within the range of illite which is 15 – 40 meq/100g (Kumari and Mohan, 2021). Raw Katiola clay has a CEC of 37.5 which increases after sodium treatment to 51.5 meq/100g. These values are higher than the standard CEC value range indicated for kaolinite (3 – 15 meq/100g) but remain lower than that of pure smectite (80 – 120 meq/100g) (Kumari and Mohan, 2021). These results justify that the clays studied are made up of a mixture of minerals. Furthermore, these CEC values are consistent with Cases et al., which indicates that smectites have a greater CEC than kaolinite or illite (Cases *et al.*, 1986). The sodium ions having occupied the interfoliar space after sodium treatment, would facilitate cation exchanges more and would justify that the CEC experiences a strong increase during the transition from K50 to K2 for Katiola clay. Gueu *et al*. (Gueu *et al.*, 2019) who made measurements on the Katiola sample reached the same observation with CEC values of 37.55 and 51.56 meq/100g after sodium treatment, below the range of Cases *et al.* (Cases *et al.*, 1986).

The results show the effect of sodium treatment on the cation exchange capacity of raw clays. Indeed, the CEC of purified clays is higher than that of raw clays, thus reflecting that the sodium saturation step improves the CEC of clays (Gueu *et al.*, 2019). The effect is more perceptible with Katiola clay in which the easily exchangeable sodium cations are inserted into the interfoliar space of the smectites it contains, after the sodium treatment. This increase is relatively small for Dabou clay. This could be due to the presence of the clay minerals it contains: kaolinite which does not have an interfoliar cation (Reynolds, 1997) and illite whose exchangeable cation is the potassium ion K^+, larger, solidly inserted and therefore making any cation exchange more difficult (Caillère *et al.*, 1982). These results confirm the interpretation of the chemical analysis, which suggested that the Dabou clay did not present a great capacity for substitution of interfoliar cations.

The slight increase observed from 14 to 16.7 meq/100g for Dabou clay is certainly related to the slight increase in the sodium level observed during the interpretation of the chemical analyses. This improvement in the CEC of clays after sodium treatment has been reported in other works (Gauly *et al.*, 2025; Messaid *et al.*, 2025; Ourari *et al.*, 2018). Sodium enrichment therefore increases the ion exchange capacity (Bohác *et al.*, 2019; Ladjal *et al.*, 2024; Marinovic *et al.*, 2017) and could potentially improve depollution applications by, for example, facilitating the adsorption of pollutants on the clay surface. From the above, purified clays (D2 and K2) containing high levels of clay minerals with better textural properties such as specific surface area, pore size and pore volume as well as high CEC values suggesting good adsorption capacities in comparison to natural raw clays were chemically activated with a view to improving their adsorption capacity. The activation conditions were presented in a previous publication (Adjoumani *et al.*, 2019).

3.2 Effects of acid activation on clays

3.2.1 Mineralogical analysis of activated clays

3.2.1.1 X-ray diffractions

The diffraction spectrum of activated Katiola clay (K2A) is shown in **Figure 11**. Analysis of the diffractogram reveals that the main clay minerals present are smectite and kaolinite. Quartz, and goethite with low intensities, are the impurities associated with these minerals. **Figure 11** also shows a shift in the characteristic peak of smectite, initially located at 7.25° (12.2 Å) towards a lower angle, located at 6.6° and which corresponds to a greater reticular distance; 13.38 Å. This observation is illustrated by the zoom of the diffractograms of K2 and K2A presented in **Figure 12**. This exfoliation, following an acid attack, was also reported by Kooli *et al*. (2005). After acid activation, they were able to synthesize organophiles (organoclays) thanks to the intercalation of a cationic surfactant in the interfoliar space of a montmorillonite (Kooli *et al*., 2005). This variation in the interfoliar distance could, according to Mokaya & Jones and Wypyxch & Satyanarayana, be due to the substitution of interfoliar ions (Na^+) by protons (H^+) and/or hydrated aluminum ions, whose radii are larger than that of hydrated sodium (Mokaya and Jones, 1995; Wypych and Satyanarayana, 2004). Indeed, the swelling increases, according to Bultel (Bultel, 2001), in the following order of cations: $K^+ < Fe^{2+} < Ca^{2+} < Na^+ < Li^+ < H^+$ and this, due to the fact that the ionic radius in the hydrated state is greater as the original atom is smaller (Pelloux *et al*., 1971).

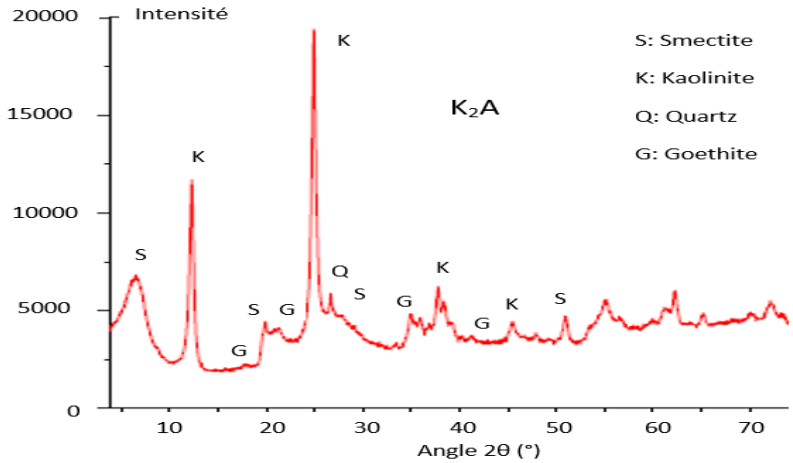


Figure 11. XRD of Katiola activated clay, K2A

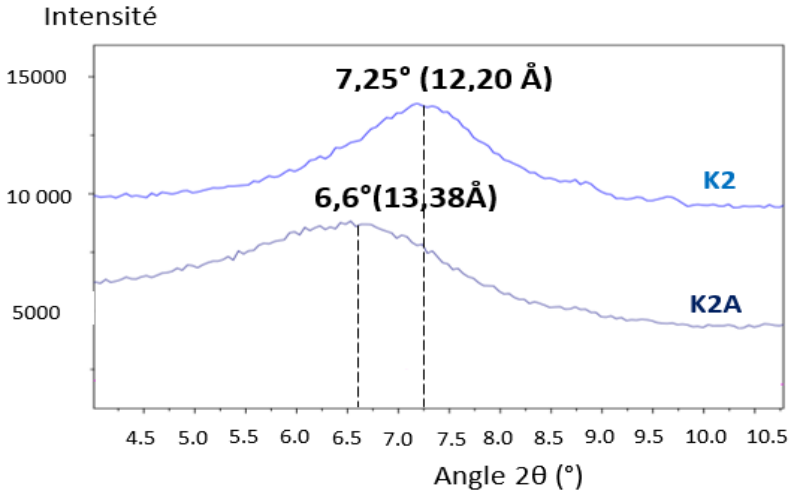


Figure 12. Zoom of the comparative diffractograms of the Katiola samples: before sodium treatment (K50), with sodium treatment (K2) and after acid activation (K2A)

Ultimately, the different treatments carried out on Katiola clay, namely sodium treatment followed by acid activation, did not disintegrate its structure; the base peak of the smectite it contains still remains present after all these treatments. The impurities have almost disappeared. The main line of smectite, which initially appeared at 7.25° (12.2 Å) for the K2 clay, remained preserved after activation (K2A) at 6.6° (13.38 Å) as illustrated by the zoom in **Figure 12**.

Other work has shown that under harsher activation conditions (higher concentration, duration and temperature), this peak decreases in intensity or disappears, indicating disintegration of the clay due to activation (Neji *et al.*, 2009). Steudel *et al.*, who brought montmorillonite into contact with 10 N sulfuric acid at 80°C for 90 hours, showed through X-ray diffraction analysis that the mineral no longer presents crystallinity and becomes completely amorphous after this acid attack (Steudel *et al.*, 2009). It would therefore be possible to say that in the present case of our study, the activation conditions used do not present any destructive effect on Katiola clay. On the contrary, activation purifies it, since the impurities have almost disappeared.

Furthermore, the shifts of the characteristic line of smectite towards 6.1° (14.48 Å) in K2 clay were also observed by Kpangni, following the sodium treatment and saturation with ethylene glycol that he carried out during his study on this same clay (Kpangni, 2009). The Hofmann-Klemen test (Hofmann and Klemen, 1950) that he carried out allowed him to specify that this smectite was made up of montmorillonite. We, by appropriating this result, and taking into account the conservation of the swelling and deflation capacity manifested by the Katiola clay in this present work, it appeared possible to us to say that the smectite contained in this clay is montmorillonite.

The diffractogram of the activated Dabou sample is presented in **Figure 13**. This figure shows, unlike the Katiola clay, a disintegration of the clay minerals of sample D2, following acid activation. The minerals that this sample contains are still present, but their intensities have become lower, notably those of the kaolinite peaks at 12.3° and 25° and the illite at 8.8°; 17.7°; 27° and 30°.

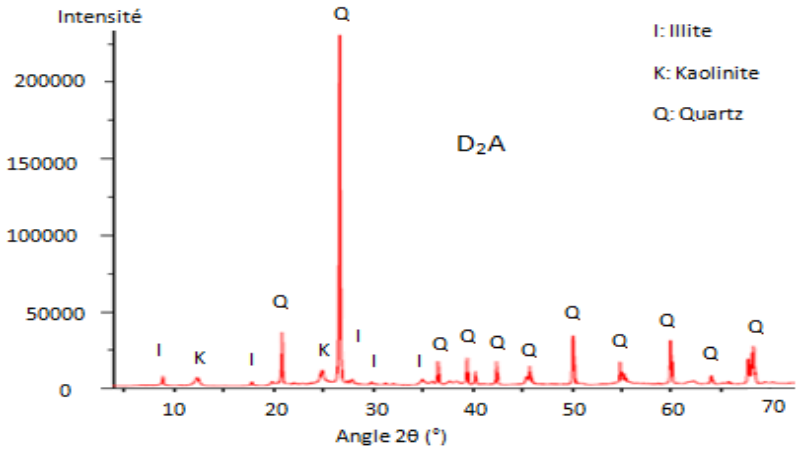


Figure 13. XRD of Dabou activated clay (D2A)

On the other hand, the peaks of impurities, notably quartz, at 20.7° and 26.7° are strongly intensified, suggesting that the silica contained in the clay minerals has passed into the form of free silica. This destructuring effect of kaolinite after acid activation at 100 °C was also reported by Aung (2014). His work focused on the decolorization of rice oil with kaolinite-rich geomaterials. The study showed that the decolorization capacity with respect to rice oil was greatly reduced under these activation conditions due to the partial or total destruction of the kaolinite structure after acid activation. This disintegration also resulted in strong leaching of aluminum from the sample with the formation of amorphous silica (Aung, 2014).

These results ultimately reveal that the sedimentation corresponding to the passage from D50 to D2 purifies it while the activation which corresponds to the passage from D2 to D2A disintegrates it. These results confirm that acid activation is strongly dependent on the clay used (Komadel, 2016; Neji *et al*., 2009; Numan and Charles, 1969).

3.2.1.2 Mineralogical composition of K2A and D2A clays

The mineralogical composition of the activated clays is presented in Table 6. This table shows the composition of samples K50, K2, D50 and D2 in addition to those of K2A and D2A. The results show a sharp drop in the kaolinite rate in the case of Dabou clay after activation, while its quartz rate experiences a strong growth. The increase in the quartz content, after activation, would be due to the disintegration of the clay minerals contained in this sample. This destructuring affects the kaolinite more in the case of the Dabou sample (D2A) since its rate experiences the greatest drop. In the case of Katiola clay, this reduction in the kaolinite rate is negligible, around 0.1% compared to 52.8% for D2A clay. This result shows that kaolinite in the presence of montmorillonite resists better acid activation (Nguetnkam *et al*., 2011). This is due to the fact that the acid attack involves ionic exchanges between compensating ions and H^+ protons (Neji *et al*., 2009). It is in the absence of swelling clay such as montmorillonite that kaolinite is destructured after acid attack as observed in the case of the material of Aung (2014), which only had kaolinite, a clay with almost zero exchange capacity.

Table 6. Mineralogical composition of the different samples

	Minerals (%)					
Samples	**Quartz**	**Smectite**	**Kaolinite**	**Illite**	**Goethite**	**Tobermorite**
K50	20.7	33.2	29.1	–	16.2	0.8
K2	6.3	51.9	39.7	–	2.1	–
K2A	4.7	54.8	39.6	–	0.9	–
D50	67	–	17	16	–	–
D2	13.3	–	66.4	20.3	–	–
D2A	70.5	–	14.6	14.9	–	–

In the case of Dabou clay, the clay minerals present, illite and kaolinite, do not promote ionic exchanges in their interfoliar space (Decarreau, 1990; Kpangni, 2009). Therefore, any acid attack directly affects the crystal lattice. These results are in agreement with those reported by Aung (2014). Ultimately, the Dabou D2A sample, obtained after acid activation of D2, is found with only 14.6% kaolinite and 14.9% illite, as clay mineral, for 70.5% quartz as impurity. On the other hand, the activation will have been beneficial for the Katiola clay which is found with 39.6% kaolinite and 54.8% smectite in the K2A sample, for 4.7% quartz and 0.9% goethite. Acid activation favoring bond breaks at the level of clay minerals (Boudjema, 2015), Katiola clay with a high level of clay minerals (**Table 6**), can thus improve its adsorption capacity, unlike Dabou clay which when disintegrating, finds itself with a reduced adsorption capacity.

3.2.2 Chemical composition

The results of the chemical analysis are presented in **Table 7**. These results show that the transition from K2 to K2A after activation causes an increase in the silica content of 17.5%, reflecting a loss of silicon from clay minerals in the form of free silica (quartz). This loss of Si is accompanied by a leaching of 25.5% of Iron and 41% of Mg. This leaching, reported in several works relating to the acid activation of clays (Boudjema, 2015; Djebbar, 2014) is the manifestation of acid attack which can lead to the destruction of the clay structure in more severe conditions (Boudjema, 2015).

Table 7. Chemical composition of the different samples before and after activation, expressed in % by mass of oxides

	SiO_2	Al_2O_3	Fe_2O_3	K_2O	MgO	CaO	Na_2O	MnO	TiO_2
K50	44.97	16.06	23.84	0.57	3.72	0.74	0.45	0.02	0.55
K2	38.18	17.46	16.13	0.16	6.64	3.75	4.44	0.00	0.30
K2A	46.29	21.15	12.02	0.03	3,92	0.10	2.80	0.00	0.15
D50	81.07	15.37	3.5	1.79	0.21	0.17	0.11	0.03	0.21
D2	55.83	34.84	2.13	1.95	0.15	0.25	0.19	0.00	0.14
D2A	82.38	16.05	1.10	1.80	0.02	0.10	0.10	0.00	0.10

The level of alumina (Al_2O_3) is experiencing growth of 17.5%. This increase in the alumina content could be the consequence of more accentuated leaching of Mg and Fe. Christidis et al. (Christidis *et al*., 1997) and Srasra (Srasra, 2002) report in this regard that the metal-oxygen bond energy is significantly greater for Al than for Mg or Fe and that Mg and Fe would therefore (Steudel *et al*., 2009), be more leached in this order than aluminum (Al). Sodium, despite a drop after activation, remains in the clay structure, probably in terms of interfoliar cations with a level of 2.80% in Na_2O oxide. Ultimately, the main elements remaining in this K2A activated clay are Al, Si, Fe, Mg and Na.

The transition from D2 to D2A after activation results in a decrease of 53.4% in the aluminum content and an increase of approximately 33% in the silica content corresponding to a probable departure of silica from the clay structure in free form. These last two results would reflect a probable collapse of the crystal lattice of the Dabou D2 clay after the acid attack and would confirm the previous results. One explanation could be linked to the possible lack of isomorphic substitutions with Dabou clay. The latter not occurring a priori, the acid attack would directly cause the leaching of the structural cations Al and Si, which leads to a breakdown of the structure of the clay and which contributes to its disintegration (Dai and Huang, 1999).

Ultimately, silicon and aluminum remain the main elements of this Dabou activated clay with a greatly reduced aluminum content. Potassium with an average oxide level of 1.8% appears as a minor element; the other elements are in the form of traces.

3.2.3 Textural properties

3.2.3.1 N_2 adsorption isotherm

Figure 14 presents the N_2 adsorption/desorption isotherms of the activated clay samples. The N2 adsorption/desorption isotherms of activated clays present similar characteristics with those of untreated natural clays and those of sodium clays.

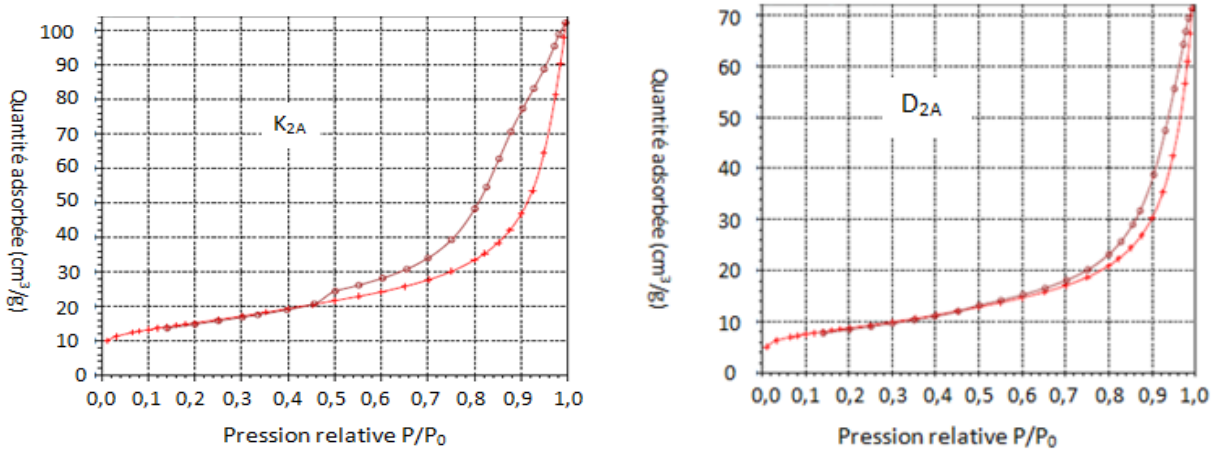


Figure 14. N_2 adsorption isotherms of activated clay from Katiola (K2A) and Dabou (D2A)

According to the classification of the International Union of Pure and Applied Chemistry (IUPAC), these clays present a type IV isotherm with H3 type desorption hysteresis loops characteristic of mesoporous materials (El-kordy *et al*., 2021) with a small pore size (Mustapha *et al*., 2019). On each of these isotherms, two typical areas of relative pressure also appear, ranging on the one hand from 0 to 0.45; highlighting the micropores, and on the other hand between 0.45 and 0.98, with desorption revealing a hysteresis characteristic of mesoporous solids. Activated Katiola clay (K2A) has the uniqueness of having a wide hysteresis upon desorption. This particularity would be due to the existence of macropores in this sample (Kpangni, 2009).

3.2.3.2 BET surface area, volume and pore size

The specific surface area of activated clays, the microporous volume and the total pore volume are grouped in **Table 8**. These values show that the specific surface area of Katiola clay increases after activation while it decreases for Dabou clay. This could be due, according to Bergaya & Lagaly, to the elimination of impurities and the multiple fragmentations that clay minerals undergo for Katiola clay (Bergaya and Lagaly, 2006). In the case of Dabou clay, the specific surface area drops because the quantity of kaolinite it possesses is greatly reduced after activation, the mineral being disintegrated into quartz whose adsorbent properties are zero (Aung, 2014). It is also observed for both samples, an increase in the size of the pores in relation to the reduction in the volume of the micropores. Conversely, the total volume increases for Katiola clay, but decreases for Dabou clay due to the sharp drop in the level of clay minerals it contains. The high surface areas of Katiola clays, associated with clay minerals (smectite and kaolinite) provide larger contact surfaces, which could potentially improve the adsorption of pollutants on the surface of these clays.

Table 8. Specific surface areas and pore volume of the clays

	Micropore surface (m^2/g)	External surface (m^2/g)	BET specific surface (m^2/g)	Pore diameter (nm)	Micropore volume (cm^3/g)	Total volume (cm^3/g)
D50	3.82	27.63	31.45	11.14	$1.5.10^{-3}$	0.087
D2	3.24	33.76	37.00	12.11	$1.1.10^{-3}$	0.114
D2A	2.13	26.25	28.38	12.6	$0.8.\ 10^{-3}$	0.074
K50	12.24	43.21	55.45	7.84	$5.2.10^{-3}$	0.109
K2	9.07	48.02	57.09	9.29	$3.8.10^{-3}$	0.125
K2A	5.08	56.25	61.33	13.12	$1.6.\ 10^{-3}$	0.155

Conclusion

The aim of this work was to understand, based on chemical, mineralogical and textural and CEC analyses, the effect of treatments carried out on clay following purification or following acid activation.

Two clay samples from two towns in Ivory Coast (Dabou and Katiola) were used for this purpose.

A first fraction of each sample, noted respectively D50 and K50, was extracted from the raw clays by wet sieving to have a particle size of 50 µm.

These first fractions were then purified to have a fine particle size of 2µm after a series of treatments (removal of organic matter, decarbonation, homoionization, washing, siphoning and drying). This second fraction was denoted respectively D2 and K2.

The third fraction noted respectively as D2A and K2A was obtained after acid activation with sulfuric acid of the purified fractions D2 and K2.

In terms of general characteristics, the results of chemical, mineralogical, textural and CEC analyzes showed that the two samples are very different in nature. The clay of Dabou (D2) is rich in kaolinite (66.4%) and illite (20.3%), as a clay mineral, while that of Katiola (K2) consists mainly of smectite (51.9%), particularly montmorillonite with a content of kaolinite (39.3%). Both samples are mesoporous with a tiny presence of micropores. The Dabou sample has a lower specific surface area and CEC compared to the Katiola sample.

Concerning the effects, for each sample, the purification treatment carried out allowed the elimination of a large part of the impurities it contained and increased their content of clay minerals, their specific surface area, as well as the volume and size of the pores. The cation exchange capacity and specific surface area increased more in the case of Katiola K2 clay.

Analysis of the results of activated clays reveals that acid activation disadvantages Dabou clay while Katiola clay is found to be even more purified, with an increasing level of clay minerals, specific surface area and CEC. This result was explained by the fact that the Dabou clay, consisting solely of kaolinite and illite, appeared to be a non-swelling clay. It therefore undergoes destructuring by leaching of these structural cations, namely aluminum (Al) and silicon (Si), which disintegrates it into free silica in the form of quartz after acid activation. On the other hand, the Katiola clay consisting mainly of smectite and kaolinite as an associated mineral appeared to be a swelling clay. It supports acid activation because, thanks to the smectite it contains, it has exchangeable cations such as sodium or magnesium, capable of being replaced by H^+ protons according to the mechanism of acid activation.

Ultimately, based on the results obtained, it was estimated that the samples studied could be used in raw form or in purified form as adsorbents for the elimination of pollutants. Katiola clay, on the other hand, being able to withstand acid activation because it is considered swelling, could improve its adsorption capacity in activated form, unlike Dabou clay, which is not swelling, which disintegrated following acid activation.

Disclosure statement: *Conflict of Interest:* The authors declare that there are no conflicts of interest.
Compliance with Ethical Standards: This article does not contain any studies involving human or animal subjects.

References

Adjia H. Z. (2012) Adsorption des métaux lourds des eaux usées par les argiles alluviales de l'Extrême-Nord Cameroun, *Thèse de Doctorat en Co-tutelle*, Universités de Lorraine/Université de Ngaoundéré, 313p

Adjoumani Y. J., Dablé P. J. M. R., Kouassi K. E., Gueu S., Assémian A. S., Yao, K. B. (2019) Modeling and Optimization of Two Clays Acidic Activation for Phosphate Ions Removal in Aqueous Solution by Response Surface Methodology, *Journal of Water Resource and Protection*, 11(02), 200-216. https://doi.org/10.4236/jwarp.2019.112012

Alujas A., Fernández R., Quintana R., Scrivener K. L., Martirena F. (2015) Pozzolanic reactivity of low grade kaolinitic clays : Influence of calcination temperature and impact of calcination products on OPC hydration, *Applied Clay Science*, 108, 94-101. https://doi.org/10.1016/j.clay.2015.01.028

Amari A., Gannouni H., Khan M. I., Almesfer M. K., Elkhaleefa A. M., Gannouni A. (2018) Effect of Structure and Chemical Activation on the Adsorption Properties of Green Clay Minerals for the Removal of Cationic Dye, *Applied Sciences*, 8(11), 2302. https://doi.org/10.3390/app8112302

Aung L. L. (2014) Preparation of activated kaolin for bleaching rice bran oil and synthetic kaolinites to assess sorption properties of these particles in relation to their morphology, *Thèse de Doctorat en Co-tutelle*, Université de Poitiers/King Mongkut's university of technology Thonburi https://doi.org/10.70675/0c5ab36ez8780z4a44za889z6923b85b9748

Bergaya F., Lagaly G. (2006) *Handbook of Clay Science, Volume 1* (1st Edition), Elsevier Science
Bergaya F., Lagaly G. (2013) *Handbook of clay science*, (2nd ed), Elsevier.
Bish D. L., Post J. E. (1989) *Modern powder diffraction*, Mineralogical society of America
Bohác P., Delavernhe L., Zervas E., Königer F., Schuhmann R., Emmerich K. (2019) Cation exchange capacity of bentonite in a saline environment, *Applied Geochemistry*, 100, 407-413. https://doi.org/10.1016/j.apgeochem.2018.12.019
Boudjema S. (2015) Synthèse de polyoxométalates à base de vanadium et/ou de ruthénium. Application à l'époxydation du cyclohexène, *Thèse de Doctorat*, Université de Tlemcen. https://dspace.univ-tlemcen.dz/handle/112/8188
Boulingui J. E., Nkoumbou C., Njoya D., Thomas F., Yvon J. (2015) Characterization of clays from Mezafe and Mengono (Ne-Libreville, Gabon) for potential uses in fired products, *Applied Clay Science*, 115, 132-144. https://doi.org/10.1016/j.clay.2015.07.029
Bouras O. (2003) Propriétés adsorbantes d'argiles pontées organophiles : Synthèse et caractérisation, *Thèse de Doctorat*, Université de Limoges
Bultel F. (2001) Prise en compte du gonflement des terrains dans le dimensionnement des revêtements des tunnels, *Thèse de Doctorat*, Ecole Nationale des Ponts et Chaussées, 298p
Caillère S., Hénin S., Rautureau M. (1982) Classification et nomenclature, *In Minéralogie des argiles: Volume 2* (2e éd.), Masson, 189p
Cases J. M., Cunin P., Grillett Y., Poinsignon C., Yvon J. (1986) Methods of analysing morphology of kaolinites : Relations between crystallographic and morphological properties, *Clay Minerals*, 21(1), 55-68. https://doi.org/10.1180/claymin.1986.021.1.05
Christidis G. E., Scott P. W., Dunham A. C. (1997) Acid Activation and Bleaching Capacity of Bentonites from the Islands of Milos and Chios, Aegean, Greece, *Applied Clay Science*, 12, 329-347
Dai J. C., Huang J. T. (1999) Surface modification of clays and clay–rubber composite, *Applied Clay Science*, 15(1-2), 51-65. https://doi.org/10.1016/S0169-1317(99)00020-4
Decarreau A. (1990) Matériaux argileux : Structure, propriétés et applications, *Société Française de Minéralogie et de Cristallographie et Groupe Français des Argiles*, 586 p, ⟨insu-00849816⟩
Dehmani Y., Bentahar I., Lgaz H., El-Kordy A., *et al*. (2026), A critical review of natural clay minerals: Structural characterization, textural properties, and adsorption mechanisms for sustainable wastewater treatment, *Materials Today Advances*, 29, 100682, https://doi.org/10.1016/j.mtadv.2025.100682
Djebbar M. (2014) Argile de Maghnia : Purification et Adsorption des Polluants, *Thèse de Doctorat*, Université d'Oran 1, 203. https://dspace.univ-oran1.dz/handle/123456789/2532
Dubinin M. M. (1979) Micropore structures of charcoal adsorbents. 1. A general characterization of micro- and supermicropores in the fissure model, *Bulletin of the Academy of Sciences of the USSR Division of Chemical Science*, 28(8), 1560-1564. https://doi.org/10.1007/BF00950967
El Bourachdi S., Ballout Y., Raza Ayub A., *et al.,* (2027). Development of Chitosan@ZnO@Ghassoul clay biohybrid beads for photocatalytic dye degradation and Cu(II) photoreduction, *Biomass and Bioenergy,* 217, Part A, 109821, ISSN 0961-9534, https://doi.org/10.1016/j.biombioe.2026.109821
El-kordy A., Elgamouz A., Lemdek E.M., Tijani N., Alharthi S.S., Kawde A.-N., Shehadi I. (2021) Preparation of Sodalite and Faujasite Clay Composite Membranes and Their Utilization in the Decontamination of Dye Effluents, *Membranes*, 12(1), 12. https://doi.org/10.3390/membranes12010012
Emeruwa E., Kouadio K. C., Kouakou C. H., Boffoue O. M., Assande A. A., Ouattara S., Coulibaly Y., Dauscher A. (2008) Caractérisation des argiles de la région d'Abidjan : Étude comparée de quelques gites et leur perspective de valorisation, *Revue Ivoirienne des Sciences et Technologie*, 11, 177-192
Fort C. I., Sanou A., Coulibaly M., Yao K. B., Turdean G. L. (2024) Green modified electrode for sensitive simultaneous heavy metal ions electrodetection, *Sensors and Actuators B: Chemical*, 418, 136326. https://doi.org/10.1016/j.snb.2024.136326

Garba Labo M. N., Ibrahim Grema M. H., Adamou Ibro, A., Kouassi E. K. A., Amadou Kiari M. N., Marou G., Yao K. B. (2026) Characterization of a clay soil from Côte d'Ivoire for use in green building, *Journal of Materials and Environmental Science*, 17(7), 1091-1108

Gauly L. P., Coulibaly M., Soro S. B., Kouadio K. S., N'Dri S. R., Sanou A., Trokourey, A. (2025) Characterization and enhanced performance of Ivorian clays as potential modifiers in carbon paste electrodes, *Discover Applied Sciences*, 7(2), 128. https://doi.org/10.1007/s42452-024-06457-1

Gueu S., Finqueneisel G., Zimny T., Bartier D., Yao B. K. (2019) Physicochemical characterization of three natural clays used as adsorbent for the humic acid removal from aqueous solution, *Adsorption Science & Technology*, 37(1-2), 77-94. https://doi.org/10.1177/0263617418811469

Haoufazane, C., Zaaboul, F., Monfalouti, H.E., Jodeh S., Azzaoui K., *et al*. (2025). Enhanced removal of C.I. direct black 80 by phosphoric acid activated plant biomass supported by DFT insights. *Sci Rep* 15, 40134 https://doi.org/10.1038/s41598-025-23886-z

Hofmann U., Klemen R. (1950) Verlust der Austauschfähigkeit von Lithiumionen an Bentonit durch Erhitzung. *Zeitschrift Für Anorganische Chemie*, 262(1-5), 95-99. https://doi.org/10.1002/zaac.19502620114

Komadel P. (2016) Acid activated clays : Materials in continuous demand, *Applied Clay Science*, 131, 84-99. https://doi.org/10.1016/j.clay.2016.05.001

Komadel P., Madejová J. (2006) Chapter 7.1 Acid Activation of Clay Minerals, In *Developments in Clay Science* (Vol. 1, p. 263-287), Elsevier. https://doi.org/10.1016/S1572-4352(05)01008-1

Kooli F., Khimyak Y. Z., Alshahate S. F., Chen F. (2005) Effect of the acid activation levels of montmorillonite clay on the cetyltrimethylammonium cations adsorption, *Langmuir*, 21, 8717-8723

Kouadio L. M., Lebouachera S. E. I., Blanc S., Sei J., Miqueu C., Pannier F., Martinez H. (2022) Characterization of Clay Materials from Ivory Coast for Their Use as Adsorbents for Wastewater Treatment, *Journal of Minerals and Materials Characterization and Engineering*, 10(04), 319-337. https://doi.org/10.4236/jmmce.2022.104023

Kouakou L. P. M.-S., Karidioula D., Manouan M. R. W., Pohan A. G. L., Cissé G., Konan L. K., Andji-Yapi J. Y. (2023) Use of two clays from Côte d'Ivoire for the adsorption of methyl red from aqueous medium, *Chemical Physics Letters*, 810, 140183. https://doi.org/10.1016/j.cplett.2022.140183

Kpangni E. B. (2009) Etude des caractéristiques minéralogiques des argiles de Katiola : Applicabilité aux problèmes d'environnement en *Côte d'Ivoire*, Thèse de Doctorat de Troisième cycle, Université de Cocody

Kpangni E. B., Andji J. Y. Y., Adouby K., Oyetola S., Kra G., Yvon J. (2008) Mineralogy of Clay Raw Materials from Cote d`ivoire : Case of the Deposit from Katiola, *Journal of Applied Sciences*, 8(5), 871-875.

Kumari N., Mohan C. (2021) Basics of Clay Minerals and Their Characteristic Properties. In G. Morari Do Nascimento (Éd.), *Clay and Clay Minerals* (p. 29), *IntechOpen*. https://doi.org/10.5772/intechopen.97672

Ladjal N., Terchi S., Debih H. (2024) Haute efficacité d'adsorption du colorant basique (cristal violet) sur la montmorillonite Algérienne, *Scientific Study & Research. Chemistry & Chemical Engineering, Biotechnology, Food Industry*, *25*(1), 001-018

Mantin I., Glaeser R. (1960) Fixation des ions cobaltihexammines par les montmorillonites acides, *Bulletin du Groupe français des argiles*, *12*(7), 83-88. https://doi.org/10.3406/argil.1960.974

Marinovic S., Ajdukovic M., Jovic-Jovicic N., Mudrinic T., Nedic-Vasiljevic B., Bankovic P., Milutinovic-Nikolic A. (2017) Adsorption of strontium on different sodium-enriched bentonites, *Journal of the Serbian Chemical Society*, 82(4), 449-463. https://doi.org/10.2298/JSC161010008M

Meite N., Konan L. K., Bamba D., Goure-Doubi B. I. H., Oyetola, S. (2018) Structural and Thermomechanical Study of Plastic Films Made from Cassava-Starch Reinforced with Kaolin and Metakaolin, *Materials Sciences and Applications*, *09*(01), 41-54. https://doi.org/10.4236/msa.2018.91003

Méité N., Zoro E. G., Doubi B. I. H. G., Sanou A., Kouakou L. P. M.-S., Fenzl N., Do Canto Lopes L. O., Konan L. K. (2024) Ageing, optical and life-cycle analysis of clay-reinforced cassava starch biocomposites, *Results in Chemistry*, *11*, 101853. https://doi.org/10.1016/j.rechem.2024.101853

Messaid B., Djemai I., Boudouh I., Robustillo M. D. (2025) Assessment of the performance of an acid-activated composite made of Na-montmorillonite Algerian clay to remove phenol and 4-chlorophenol from water, *Desalination and Water Treatment*, 322, 101088. https://doi.org/10.1016/j.dwt.2025.101088

Mokaya R., Jones W. (1995) Pillared Clays and Pillared Acid-Activated Clays : A Comparative Study of Physical, Acidic Properties, In *Journal of Catalysis* (Vol. 153, p. 76-85). https://doi.org/002-9517/95%2056.00

Morgan D. A., Shaw D. B., Sidebottom M. J., Soon T. C., Taylor R. S. (1985) The function of bleaching earths in the processing of palm, palm kernel and coconut oils, *Journal of the American Oil Chemists' Society*, *62*(2), 292-299. https://doi.org/10.1007/BF02541394

Murray H. H. (2007) *Applied clay mineralogy : Occurrences, processing and application of kaolins, bentonites, palygorskite-sepiolite, and common clays* (1. ed). Elsevier

Mustapha S., Ndamitso M. M., Abdulkareem A. S., Tijani J. O., Mohammed A. K., Shuaib D. T. (2019) Potential of using kaolin as a natural adsorbent for the removal of pollutants from tannery wastewater, *Heliyon*, 5(11), e02923. https://doi.org/10.1016/j.heliyon.2019.e02923

Neji S. B., Trabelsi M., Frikha M. H. (2009) Activation d'une argile smectite tunisienne à l'acide sulfurique : Rôle catalytique de l'acide adsorbé par l'argile, *Journal de la Société Chimique de Tunisie*, 11, 191-203

Nguetnkam J. P., Kamga R., Villiéras F., Ekodeck G. E., Razafitianamaharavo A., Yvon J. (2011) Alteration of cameroonian clays under acid treatment. Comparison with industrial adsorbents, *Applied Clay Science*, 52(1-2), 122-132. https://doi.org/10.1016/j.clay.2011.02.009

Nshimiyimana P., Fagel N., Messan A., Wetshondo D.O., Courard L. (2020) Physico-chemical and mineralogical characterization of clay materials suitable for production of stabilized compressed earth blocks, *Construction and Building Materials*, 241, 118097. https://doi.org/10.1016/j.conbuildmat.2020.118097

Numan A., Charles E. W. (1969) Kinetics of acid dissolution of playgorskite (attapulgite) and sepiolite, *Clays Clay Miner*, 17, 169-178

Ourari A., Tennah F., Ruíz-Rosas R., Aggoun D., Morallón E. (2018) Bentonite Modified Carbon Paste Electrode as a Selective Electrochemical Sensor for the Detection of Cadmium and Lead in Aqueous Solution, *International Journal of Electrochemical Science*, 13(2), 1683-1699. https://doi.org/10.20964/2018.02.35

Pelloux P., Dabin B., Fillmann G., Gomez P. (1971) Methodes de determination des cations échangeables et de la capacité d'échange dan sles sols, *Initiations - Documentations techniques*, (17)

Rehman M. U., Manan A., Uzair M., Khan A. S., Ullah A., Ahmad A. S., Wazir A. H., Qazi I., Khan M. A. (2021) Physicochemical characterization of Pakistani clay for adsorption of methylene blue : Kinetic, isotherm and thermodynamic study, *Materials Chemistry and Physics*, 269, 124722. https://doi.org/10.1016/j.matchemphys.2021.124722

Reynolds J. M. (1997) An Introduction to Applied and Environmental Geophysics (1st Edition), *John Wiley and Sons Ltd*.

Sako I., Kouame A. N., Ossonon D. B., Kinimo K. C. (2025) Evaluation of the physico-chemical properties of two clays for use as adsorbents in wastewater treatment, *Journal of Materials and Environmental Science*, 16(9), 1709-1720

Sanou A., Coulibaly M., N'Dri S. R., Tămaș T. L., Bizo L., Frentiu T., Covaci E., Abro K. D. M., Dablé P. J.-M. R., Yao K. B., Fort C. I., Turdean G. L. (2024) Raw clay material-based modified carbon paste electrodes for sensitive heavy metal detection in drinking water, *Journal of Materials Science*, 59(30), 13961-13977. https://doi.org/10.1007/s10853-024-09945-2

Sanou I., Senou I., Ouedrogo H., Sawadogo L., Sanou A., Nacro H. B. (2026) Physicochemical characterization of biochar and study of their effect on the bioavailability of heavy metals in soil from Burkina Faso, *Journal of Materials and Environmental Science*, 17(8), 1242-1257

Ségalen P. (1969) Contribution à la connaissance de la couleur des sols à sesquioxydes de la zone intertropicale : Sols jaunes et sols rouges, *Cah. ORSTOM Sér Pédol,* 7(2), 12

Seghairi N., Achour S. (2003) Influence du temps et du taux d'activation de la bentonite sur l'adsorption de l'aniline, *Larhyss Journal*, (2), 115-125

Sing K. S. W., Everett D. H., Haul R. A. W., Moscou L., Pierotti R. A., Rouquerol J., Siemieniewska T. (1982) Reporting Physisorption Data for Gas/Solid Systems, *Pure and Appl. Chem*, 54(11), 2201-2218. https://doi.org/10.1002/9783527610044.hetcat0065

Soro S. B., Coulibaly M., Gauly L. P., N'Dri, S. R., Sanou, A., & Trokourey, A. (2023). Characterization of Clay Materials from Côte d'Ivoire : Possible Application for the Electrochemical Analysis. *Journal of Materials Science Research*, *12*(1), 51-64. https://doi.org/10.5539/jmsr.v12n1p51

Srasra E. (2002) Argile et acidité. Mécanisme de l'activation acide et propriétés résultantes, *Thèse de Doctorat*, Université de Tunis

Steudel A., Batenburg L. F., Fischer H. R., Weidler P. G., Emmerich K. (2009) Alteration of non-swelling clay minerals and magadiite by acid activation, *Applied Clay Science*, 44(1-2), 95-104. https://doi.org/10.1016/j.clay.2009.02.001

Surez B., Robert M., Elsass M., Pozas M. F. (1995) Evidence of a precursor in the neoformation of palysgorskite. New data by analytical electron microscopy, *Clay Miner*, 29, 255-264

Thiry M., Carrillo N., Franke C., Martineau N. (2013) Technique de préparation des minéraux argileux en vue de l'analyse par diffraction des Rayons X et introduction à l'interprétation des diagrammes, *HAL*, (hal-00872214), 39

Tra B. G. A., Bamba D., Méité N., Kouamé A. N., Coulibaly M., Konan K. L. (2026) Physico-Chemical, Mineralogical, and Morphological Characterizations of Three Clays from Côte d'Ivoire with a View to Their Use in Adsorption, *Journal of Materials Science and Chemical Engineering*, 14(04), 31-52. https://doi.org/10.4236/msce.2026.144003

Wypych F., Satyanarayana K. G. (Éds.). (2004) Clay surfaces : Fundamentals and applications: Volume 1 [Electronic resource], *Elsevier Academic Press*